Journal of Chromatography, 506 (1990) 547–561
Elsevier Science Publishers B.V., Amsterdam — Printed in The Netherlands

CHROMSYMP. 1771

Hydrodynamic chromatography of macromolecules on small spherical non-porous silica particles

G. STEGEMAN, R. OOSTERVINK, J. C. KRAAK* and H. POPPE
Laboratory for Analytical Chemistry, University of Amsterdam, Nieuwe Achtergracht 166, 1018 WV Amsterdam (The Netherlands)
and
K. K. UNGER
Institut für Anorganische und Analytische Chemie, Johannes Gutenberg Universität, Joh. Joachim Bercher-Weg 24, D-6500 Mainz (F.R.G.)

SUMMARY

Non-porous silica spheres with sizes in the range 1.4–2.7 μm were applied as packings for the hydrodynamic chromatography (HDC) of macromolecules. Highly efficient columns, with a reduced plate height below 2, were packed with these small particles. Up to molecular weights of 10^6 the elution behaviour of polystyrenes agreed very well with existing theoretical models. However, for larger polystyrenes the flow-rate exerted an influence on the relative peak positions. The applicability of HDC to rapid separations of soluble macromolecules and inorganic colloids was demonstrated.

INTRODUCTION

In hydrodynamic chromatography (HDC), soluble macromolecules or particles are separated on basis of their size. In a non-uniform flow profile such as occurs in a packed bed or an open capillary, large molecules are excluded from the low-velocity flow regions near the wall. As a result, large molecules experience a larger mean velocity than smaller molecules which can approach the wall more closely[1–7]. Significant differences in migration rate occur only when the ratio of the solute radius to that of the flow channels (the aspect ratio), is larger than 0.01. However, when this ratio exceeds 0.3, solutes cannot migrate through the column. In practice, it appears that the working range is between the retention time for the low-molecular-weight marker, t_0, and $0.75t_0$ for the molecules or colloids with the largest accessible size. This means that the peak capacity is dependent solely on the magnitude of peak broadening.

In the early days, HDC was performed in columns packed with non-porous particles larger than 20 μm (ref. 3), which limited its application to very large solutes. Further extension of HDC to smaller solutes was thwarted by the lack of smaller

0021-9673/90/$03.50 © 1990 Elsevier Science Publishers B.V.

non-porous packing particles. As open tubes were available with a wide range of diameters, capillary HDC became attractive. Open capillaries offer the additional advantages that the flow channels are well defined and good permeability allows the use of long columns. Some applications of capillary HDC for the analysis of particles with sizes in the micrometre range have been reported[5,6].

An interesting area of HDC is in the size range 0.001–1 μm, which includes polymers with molecular weights up to $2 \cdot 10^7$. This size range is still difficult to cover with size-exclusion chromatography (SEC). To apply capillary HDC to this group of polymers, the flow channels have to be about 1 μm or smaller to obtain a sufficiently large aspect ratio. Tijssen *et al.*[8] managed to apply fused-silica microcapillaries with diameters down to 1 μm to the HDC of polystyrenes. However, the practical application of open tubes with such small diameters is still limited, because of the extreme requirements placed on the magnitude of the external peak broadening by injection and detection. Tijssen *et al.*[8] solved this problem to some extent by extreme miniaturization of the injection and detection systems. However, as a result, relatively high sample concentrations had to be injected to detect the samples, which may seriously affect the migration rate of the solutes. In addition, capillary HDC does not have any (micro)preparative prospects.

Recently, non-porous spherical silica particles down to 1 μm in size became available[9]. Columns packed with these particles provide flow channels that are even smaller than those reported in capillary HDC. For example, in a column packed with 1.5-μm particles, the interstitial channels are about 0.6 μm in diameter. Still, the void volume of a packed column can be so large that common or slightly modified high-performance liquid chromatographic (HPLC) equipment can be used[10]. A disadvantage of packed-column HDC is that the geometry of the flow channels in a packed bed is less well defined than in open capillary tubes, which complicates the interpretation of chromatographic results in terms of the physical behaviour of molecules or colloids.

When packing particles of about 1 μm are used, HDC enters the molecular weight range traditionally covered by SEC. Although the ranges of application will probably never coincide, an overlapping area already exists between the current lower limit of HDC (weight-average molecular weight, M_w, 10^4) and the upper limit of SEC (M_w 10^6). In this range, HDC can be superior to SEC because of the extremely small band spreading, owing to the small size of the packing particles and to the absence of an intraparticle mass-transfer term. Moreover, SEC traces are more difficult to interpret, partly because HDC effects may also be present[11,12].

In this study, the applicability of 1.4–2.7-μm non-porous spherical silica particles as a packing for the HDC of soluble polymers and colloidal particles was investigated. The column performance and the elution behaviour of polystyrenes were studied. Some preliminary results on the HDC of colloidal silica particles are reported.

EXPERIMENTAL

Apparatus

The chromatographic set-up consisted of a constant-flow pump (Model 8500; Varian, Palo Alto, CA, U.S.A.), a pneumatically driven injection valve (Type 7413; Rheodyne, Berkeley, CA, U.S.A.) equipped with a 0.5-μl internal sample loop,

a variable-wavelength UV detector (Spectroflow 757; Kratos, Ramsey, NJ, U.SA.) and a potentiometric recorder (Kompensograph 3; Siemens, Karlsruhe, F.R.G.). The detection cell of the UV detector was adapted by replacement of the original flow cell by a 100-μm I.D. fused-silica capillary, the protective polyimide layer of which was burned off. The amount of light that was transmitted through the quartz tube wall but did not pass through the liquid stream was minimized by means of an adjustable slit[13]. The fused-silica capillary, which had a length of about 12 cm, was coupled directly to the column outlet. The wavelength setting was 210 nm for polystyrene detection and 200 nm for colloids. Between the sample introduction part and the injection valve a precolumn filter unit was installed, containing a 0.5-μm filtering frit (Upchurch Scientific, Oak Harbor, WA, U.S.A.). Columns were made of 316 stainless steel and had dimensions of 150–250 × 4.6 mm I.D. Column end-fittings were installed with removable frits with 0.5-μm pores (VICI, Houston, TX, U.S.A.). A dual-stage electron microscope (Model DS 130; ISI, Tokyo, Japan) was used for the determination of the packing particle size.

Materials

Analytical-reagent grade tetrahydrofuran (THF), methanol and carbon tetrachloride (Merck, Darmstadt, F.R.G.) were used without further purification. Water was deionized through a PSC filter assembly (Barnstead, Boston, MA, U.S.A.). Prior to use, the eluents were filtered by vacuum suction over a 0.5-μm filter (Type FH and VHLP; Millipore, Bedford, MA, U.S.A.).

Polystyrene (PS) standards with weight-average molecular weight (M_w) 0.5–2750 kilodalton and stated polydispersities ranging from 1.04 to 1.18 were obtained from Merck. Polystyrenes with M_w of 300–20 150 kilodalton and stated polydispersities from 1.03 to 1.30, were purchased from Macherey-Nagel (Düren, F.R.G.). The fumed silica nanospheres were obtained from Cabot (Tuscola, IL, U.S.A.).

Column preparation

The columns were packed by means of the slurry-packing technique, using methanol as both a slurry liquid and a driving liquid. A slurry was prepared by common ultrasonification of 10% (w/w) of the packing particles in methanol. Agglomerates of particles were removed by sedimentation. Prior to packing, the ultrasonic treatment was performed once more for 20 min to obtain a homogeneous suspension. During packing, a constant flow-rate of about 3 ml/min was maintained by smoothly increasing the pressure up to a final value of 700–900 bar, depending on the particle diameter and the column length. At the final pressure, the column was flushed with another 60 ml of methanol. After the pump had been switched off, the pressure was allowed to drop to zero before the column was disconnected. Finally, the column was equilibrated with the mobile phase until a stable detector baseline was obtained.

Sample preparation

The polystyrene sample solutions were prepared by carefully adding THF to the polymer up to a concentration of 0.01–0.03% (w/w). The samples were left overnight to swell and dissolve slowly. The colloid sample was prepared by suspending 14-nm silica nanospheres, 0.5% (w/w) in the mobile phase (dilute ammonia, pH 8.9). Aggregates were removed by filtration over a 0.2-μm filter (Millipore).

Chromatography

The non-porous spherical silica packing particles were prepared according to the method described by Unger and Giesche[9]. All chromatographic experiments were carried out at room temperature (23 ± 2°C). The reported values are the means of at least three measurements. The polystyrenes were injected together with the marker (toluene) unless peak overlap necessitated injection of the polymer and the marker separately.

THEORY

Various theoretical models have been developed to describe the migration of solutes in HDC[8,14–19]. Most of these models include solute–wall interactions and therefore lead to complex expressions for the migration rate. Athough solute–wall interactions are of importance in HDC[18,20,21], we assume they are absent in our experiments on the elution behaviour of polystyrenes. On that condition, a general equation is valid for the migration rate, expressed by a relative quantity τ as function of the aspect ratio λ:

$$\tau = (1 + 2\lambda - C\lambda^2)^{-1} \tag{1}$$

where $\tau = t_p/t_m$ and $\lambda = r_i/R$, t_p and t_m are the retention times of the polymer and the low-molecular-weight marker solute, respectively, r_i is the radius of the solute molecule and R is the radius of the flow channel.

For the simplest model based on a Poiseuille flow profile, the value of C would be 1. For secondary effects such as rotation, C departs from 1 and ranges between 1 and 5.3 in the different models, depending on the type of solute, *e.g.*, permeable or hard-sphere polymers[8].

In contrast to capillary HDC, the geometry of the flow channel in a packed bed is not well defined, which makes it difficult to express λ. In order to apply the various models to packed beds, the hydraulic radius R_0 is often used. This is the radius of a capillary having the same surface-to-volume ratio as the packed bed under study. For spherical particles, the value of R_0 can be calculated from the particle size, d_p, and the bed porosity ε, according to[22]

$$R_0 = \frac{d_p}{3} \cdot \frac{\varepsilon}{1 - \varepsilon} \tag{2}$$

In a packed bed the radius of the flow channel R is then replaced by R_0.

By using eqn. 1, an expression can be derived for the resolution R_s between two solutes i and j eluting close together[10]:

$$R_s = \frac{t_j - t_i}{\sigma_{t_i}} = (\alpha - 1)(1 - C\lambda)\lambda\tau\sqrt{N} \tag{3}$$

where σ_{t_i} is the standard deviation of peak i, α is the ratio of the radii of solutes i and j, where $r_i > r_j$, and N is the number of theoretical plates.

RESULTS AND DISCUSSION

The main characteristics of the investigated columns are summarized in Table I. In all experiments the porosities ε of the columns were calculated from the void volume as determined by weighing the columns filled with pure solvents of different densities. The porosities calculated in this way agreed very well with those calculated from the retention times of the marker and the flow-rate settings.

The flow resistance parameters ϕ for the HDC columns in Table I are about half those usually obtained for porous particles. This results from the fact that ϕ is calculated from the migration velocity of a non-sorbed solute rather than from the velocity in interparticle space. With porous particles these two velocities differ by a factor of about 2, whereas in our case they are the same. Consequently, pressure limitations in HDC on non-porous particles are not as severe as in HPLC on porous particles.

Column efficiency

When using 1–3-μm non-porous particles in HDC, plate heights of a few micrometres can be expected[10]. To conserve the high column efficiency in the chromatographic system, severe demands are placed on the magnitude of the external peak broadening. For instance, the volume standard deviation σ_v for the marker solute on a 150 × 4.6 mm I.D. column filled with 1-μm particles and having a reduced plate height of 2 would be 3.5 μl. The external contributions to zone dispersion, $\sigma_{v,ext}$, should then not exceed 1.7 μl. In our case, $\sigma_{v,ext}$ could be minimized by using both a small injection and detection cell volume and small-diameter connecting tubes. The total external contribution was measured after connecting the injection valve directly to the detector by means of a zero-dead-volume union. In the flow-rate range from 2.7 to 17 μl/s (corresponding to a linear velocity range of 0.4–2.6 mm/s for the columns used), $\sigma_{v,ext}$ was between 0.7 and 1.3 μl. It was therefore concluded that the measured plate height would hardly be affected by extra-column band broadening.

As phase distributions are absent in HDC, existing plate-height theories[23–25] predict that dispersion is determined exclusively by longitudinal molecular diffusion and convective mixing. At high linear velocities, molecular diffusion has a negligible influence on the overall dispersion, and a constant plate height is predicted, irrespective of the value of the molecular diffusion coefficient. The dispersion due to longitudinal molecular diffusion occurring at small linear velocities depends on the

TABLE I

COLUMN CHARACTERISTICS

Column	*L (mm)*	d_p (μm)[a]	ε	R_0 (μm)[b]	ϕ[c]
A	150	1.40	0.380	0.286	447
B	250	1.91	0.395	0.416	509
C	150	2.67	0.385	0.561	417

[a] SEM measurements.
[b] According to eqn. 2.
[c] According to $\phi = Pd_p^2/(\langle v \rangle \eta L)$.

molecular weight of the polymer. Consequently, the higher the molecular weight, the smaller will be the linear velocity at which the minimum in the plate height curve is reached.

Fig. 1 shows the plate heights obtained for three solutes of different molecular weights and two particle sizes. It can be seen that the minimum of the plate height curve shifts to lower velocities for larger polymers. It appears that extremely efficient columns can be prepared with the non-porous particles used. For column C (Fig. 1a), minimum plate heights of 3.6 μm for toluene and PS 2.2 kilodalton and 3.8 μm for 336 kilodalton were found. This corresponds to a minimum reduced plate height of 1.3–1.4. The optimum plate number was thus 42000 for the 150-mm column. Measured plate heights for column A (Fig. 1b) were even lower, in accordance with theory. The minimum value of 2.2 μm for PS 2.2 kilodalton (N = 68000) provides a reduced plate height of 1.6, while the minimum for toluene had not been reached at the highest accessible velocity. In contrast to theoretical prediction, the curves for PS 336 kilodalton at high linear velocities do not coincide with those obtained with PS 2.2

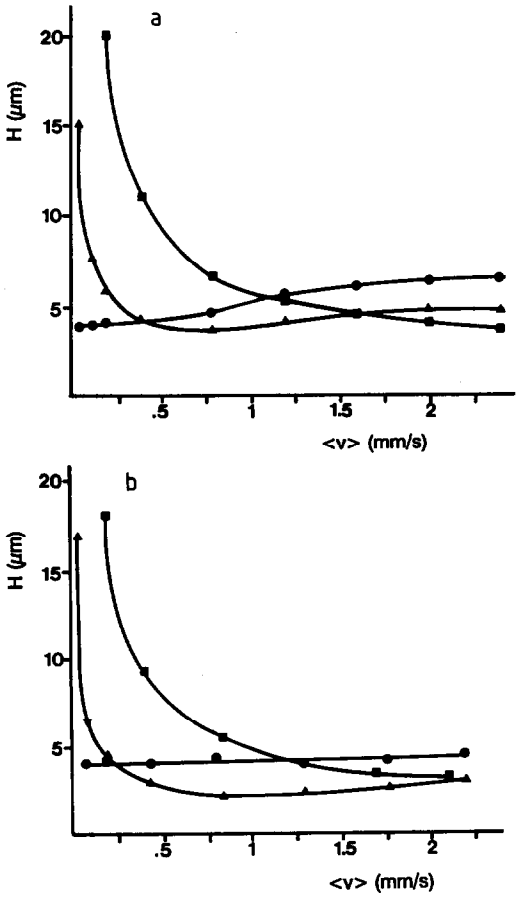

Fig. 1. Plate height, H, *versus* linear velocity, $\langle v \rangle$, of some standards on (a) column C and (b) column A. Solutes: ●, = PS 336 kilodalton; ▲ = PS 2.2 kilodalton; ■ = toluene.

kilodalton and toluene. The curves are almost flat and show a larger plate height value than expected. This deviation may be attributed to the polydispersity of the sample.

Knox and McLennan[26] investigated the effect of the polydispersity of polymer standards in SEC. They found that broadening due to polydispersity could be substantial, especially for polymers eluting in the linear part of the calibration graph. They stated that the true plate height can be calculated from the measured plate height, the polydispersity of the sample and the slope of the calibration graph. When, for example, this approach is applied to the plate height of PS 336 kilodalton on column A, using the manufacturer's data on polydispersity ($M_w/M_n = 1.03$, where M_n is the number-average molecular weight), surprisingly the corrected plate height is negative. Assuming now that the observed plate height is determined solely by the polydispersity of the sample (*i.e.*, the column has zero plate height), the upper limit of polydispersity can be calculated. The value thus obtained ($M_w/M_n < 1.01$) is considerably lower than that given by the manufacturer. At present we are not able to decide whether indeed our polymer samples are much more monodisperse, or whether on the contrary there is some experimental artefact or physical phenomenon that leads to the remarkably sharp peaks that we observed.

Elution behaviour of polystyrenes

An estimate of the radius of the dissolved polymer is needed for the application of eqn. 1. For random coil polymers several expressions exist based on the radius of gyration or the hydrodynamic radius. These expressions can be summarized by the general relationship

$$r_i = aM_w^b \tag{4}$$

Tijssen *et al.*[8] made a strong case for the use of the so-called effective polymer radius[27,28], equal to 0.886 times the radius of gyration, and we followed their proposal. Substitution of the effective polystyrene radius in THF and the hydraulic radius of the packed bed (eqn. 2) in the definition of λ leads to

$$\lambda = \frac{1.23 \cdot 10^{-5} \cdot M_w^{0.588}}{R_0} \tag{5}$$

To predict the migration rate of the polymers theoretically, the parameter C in eqn. 1 remains to be established. Therefore, two theoretical models yielding different C values are discussed. In the first model, after DiMarzio and Guttman[1,2] (DG model), the hydrodynamic behaviour is described for free-draining permeable, rotating spheres in a parabolic flow field. The DG model yields a C value of 2.70. The second model, according to Brenner and Gaydos[29] (BG model), is more refined and leads to $C = 4.89$. Tijssen *et al.*[8] modified the BG model for free-draining permeable spheres and obtained $C = 5.26$. In the discussion of experimental results the two values for C, *i.e.*, 2.70 and 5.26, are used as reference points. Differences between the two migration models appear only at higher aspect ratios ($\lambda > 0.03$). Therefore, to decide which model best fits to the packed columns used in this study, it is essential to include the τ values of high-molecular-weight polymers.

Fig. 2 shows the elution of various polystyrenes on three columns filled with differently sized packing particles. Dashed lines in these figures are drawn for $C = 3.7$. The value of C does not matter too much (see Figs. 3 and 4) for the high-τ end of the figure, which will be discussed first. The drawn lines were obtained by using eqn. 1, calculating the aspect ratio with eqn. 5 and using a d_p from scanning electron microscopic (SEM) measurements. Therefore, no adjustable parameters are necessary for calibration in this part of the figure. The parameter λ, and its relation to τ, appear to be so well established that the elution can be predicted strinkingly well. We may therefore conclude that the packed bed can indeed be represented in terms of an equivalent capillary model. In addition, the results indicate that the expression for the polymer radius leads to the correct description of hydrodynamic behaviour in packed beds, similarly to that observed by Tijssen *et al.*[8] for open capillaries.

The C value of 3.7 was chosen because it was found previously[10] with 2.1-μm particles to give the best fit of the experimental results. However, although the 1.4-μm data do coincide with the line for $C = 3.7$, the data for $d_p = 1.9$ and 2.7 μm deviate significantly for large molecular weights. Polymers with molecular weights larger than about $2 \cdot 10^6$ all eluted later than predicted by theory. In addition, a minimum τ value eseemed to exist for columns B and C at which all polymers with molecular weights $> 2 \cdot 10^6$ coeluted. We checked whether this could be a retardation effect caused by the small frit pores. However, replacement of the 0.5-μm frit in column C by a 2.0-μm frit had no significant effect on the elution time of the large polymers. Changing the linear velocity of the eluent, on the other hand, proved to affect the elution behaviour significantly. This effect was studied in more detail for columns A and B.

The results of measurements on the flow-dependent elution behaviour are given in Table II. As can be seen, no significant velocity effect on τ is observed for $M_w < 1000$ kilodalton in the investigated velocity range. This result is in accordance with previous

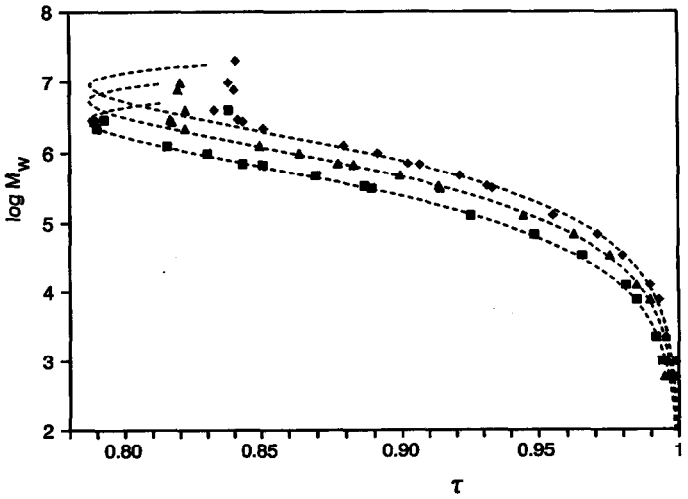

Fig. 2. Elution behaviour of PS in THF for different packing diameters: ■ = 1.40 μm, column A; ▲ = 1.91 μm, column B; ◆ = 2.69 μm, column C. Linear velocity $\langle v \rangle \approx 0.87$ mm/s. Theoretical curves according to eqn. 1 where $C = 3.7$.

TABLE II

DEPENDENCE OF τ OF SOME HIGH-M_w POLYSTYRENES ON THE LINEAR VELOCITY $\langle v \rangle$ ON COLUMNS A AND B

Column	$M_w \cdot 10^6$	$\langle v \rangle$ *(mm/s)*		
		0.87	*0.43*	*0.21*
A	0.68	0.8504	0.8506	0.8503
	1.26	0.8152	0.8110	0.8107
	2.20	0.7900	0.7737	0.7722
	2.95	0.7927	0.7674	0.7583
	4.00	0.8379	0.7668	0.7436
B	0.68	0.8827	0.8827	0.8829
	1.26	0.8494	0.8452	0.8440
	2.20	0.8218	0.8105	0.8089
	2.95	0.8164	0.7993	0.7907
	4.00	0.8220	0.7872	0.7743
	9.80	0.8200	0.7878	0.7647

work[10]. However, for larger polystyrenes reduction of the flow-rate caused a decrease in τ. Simultaneously, peak broadening and peak tailing decreased in the chromatograms. The larger the polymer size, the more prominent these effects were. At lower velocities, the observed minimum τ values had declined and coelution of different polymers was diminished.

An explanation of the observed results might be given in terms of shear degradation of the polymers. It is well known that shear degradation increases with increasing polymer size and linear velocity[30,31], although quantitative predictions are difficult[32]. Degradation of polymers causes peaks to shift towards lower molecular weights whereas peak broadening and tailing increase, in accordance with our observations. Although shear degradation seems to be an acceptable explanation for the observed phenomena, alternative explanations might be considered. Giddings[33], for instance, considered that in packed columns retardation effects might occur for large polymers owing to collisions against the wall and trapment in crevices and apertures. These effects also depend on polymer size and flow velocity. Also, concentration[34,35] and viscosity effects[36] may be of importance for these large polymers. More research has to be performed in order to explain the observed results unambiguously.

A dependence of τ on the linear velocity is not accounted for in the theoretical models. When we assume that interfering effects occur only at high velocities, we should compare the theoretical models with our low-velocity measurements. In Figs. 3 and 4, the DG model, the BG model and experimental results at different linear velocities are plotted. It can be seen that the modified BG model corresponded with the iexperimental results only in the low-molecular-weight range. Flow reduction even worsened the agreement. On the other hand, the DG model corresponded reasonably well up to molecular weights of about 10^6. On flow reduction the fit of the DG model improved considerably for $M_w > 1000$ kilodalton. At the lowest flow-rate setting, the DG model almost matched the whole experimental calibration graph. Only around the

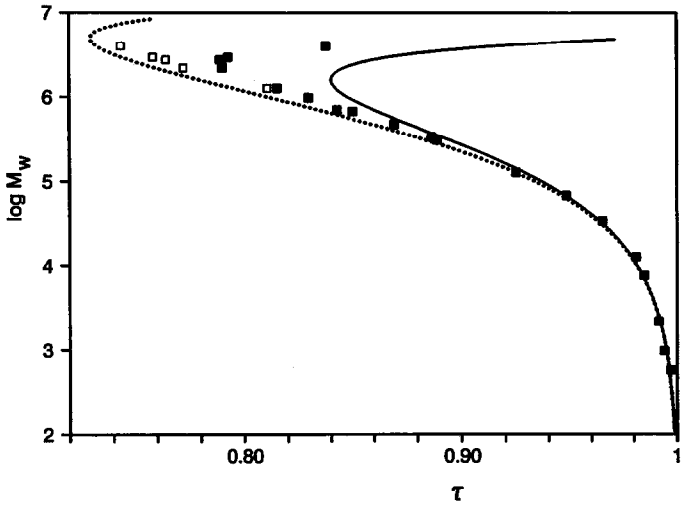

Fig. 3. Theoretical calibration graphs and experimental points for column A at different linear velocities. Theoretical: dotted line, DG model; solid line, BG model. Experimental: (■) $\langle v \rangle$ = 0.87 mm/s; (□) $\langle v \rangle$ = 0.21 mm/s.

backward turn of the calibration graph did the theoretical line differ from the experimental points. Whether the lowest τ values predicted by the DG model will finally be reached at even lower linear velocities is still to be determined. More research, preferably with the use of smaller packing materials, should be performed.

Both theoretical models assume infinite dilution of the polymer sample. At high solute concentrations, elution of high-molecular-weight polymers may suffer from concentration and viscosity effects. The theoretical models are then no longer valid. In

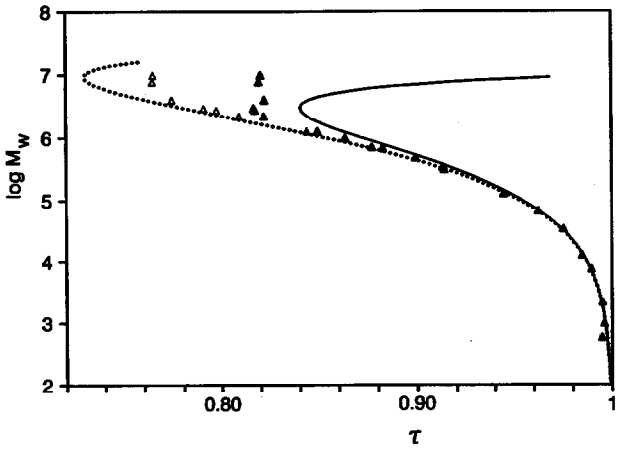

Fig 4. Theoretical calibration graphs and experimental points for column B at different linear velocities. Theoretical: dotted line, DG model; solid line, BG model. Experimental: (▲) $\langle v \rangle$ = 0.87 mm/s; (△) $\langle v \rangle$ = 0.21 mm/s.

micro-capillary HDC, Tijssen *et al.*[8] could not make an experimental distinction between the DG and BG models, because they had to use high solute concentrations (1 mg/ml) to obtain any detectable peaks. Indeed, the peaks they observed for the large polymers were triangular and elution was probably considerably affected. In our experiments, detection problems were of less importance, so more dilute samples could be used (0.1–0.3 mg/ml). We were therefore much better equipped to test the validity of the two theoretical models and the available evidence strongly indicates a preference for the DG model ($C = 2.70$).

For molecular weights up to 10^6, the elution behaviour appeared to be independent of the flow-rate under the selected circumstances. For these samples a universal calibration graph was drawn by plotting log λ against τ for three columns (Fig. 5). It appears that all experimental points fall along one line with very little scatter. This illustrates that, although columns may be prepared with different-sized packing materials and with different packing pressures, hydrodynamic behaviour can be described by one universal calibration equation. The only remaining adjustable parameter in this equation is C, which at a later stage may be unequivocally determined.

Separation of polystyrene mixtures

Fig. 6 shows rapid separations of a mixture of polystyrenes on columns A (Fig. 6a) and C (Fig. 6b). Column A appears to be well suited to separate this mixture because the whole molecular weight range (τ between 0.77 and 1) is covered. On column C, R_0 is larger, resulting in smaller aspect ratios and higher τ values for all components of the polymer sample. The peaks therefore elute closer together and the resolution deteriorates (τ between 0.83 and 1).

From eqn. 3, it is clear that the resolution improves with higher plate numbers. Only for this reason may the smallest peak widths be expected for separations on

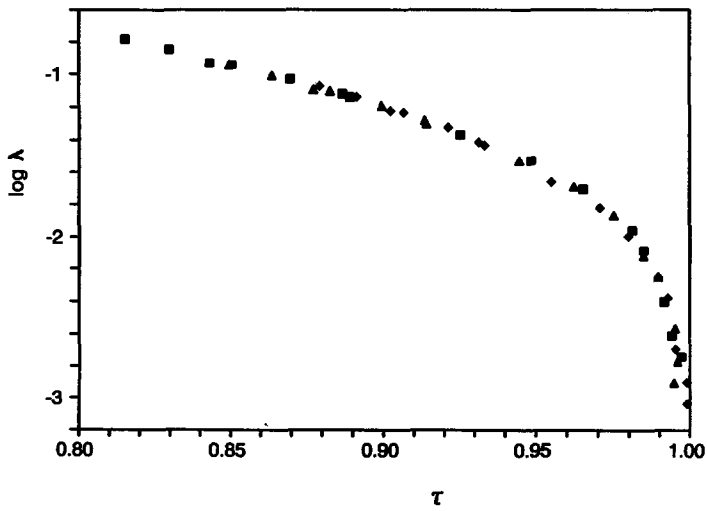

Fig. 5. Universal HDC calibration graph for polystyrenes: ■ = column A; ▲ = column B; ◆ = column C. Linear velocity range: 0.21–0.87 mm/s.

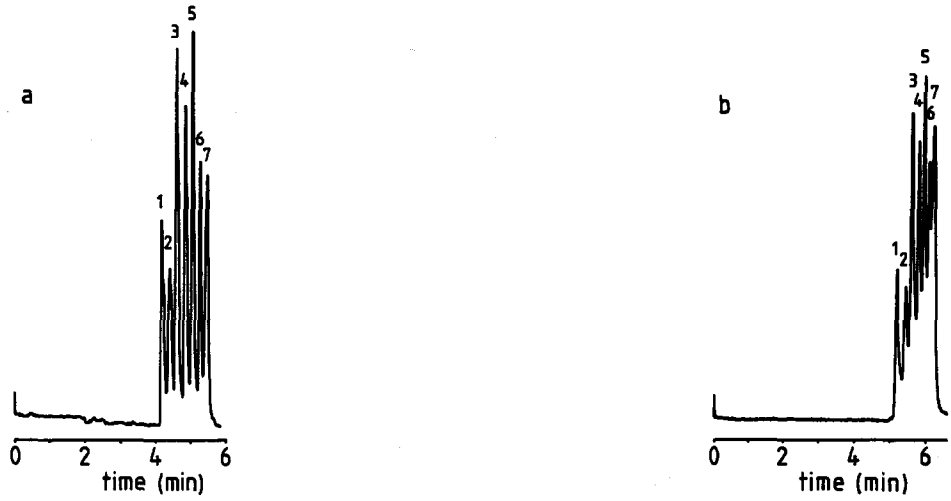

Fig. 6. HDC separation of PS standards on (a) column A and (b) column C. Sample containing: (1) 2750-; (2) 1260-; (3) 700-; (4) 310-; (5) 127-; (6) 34.5-kilodalton PS; and (7) toluene.

column A. From a previous paragraph, however, it can be concluded that this effect is largely obviated by the polydispersity of the polymer samples. To visualize the effect of polydispersity, the chromatogram shown in Fig. 6a was computer simulated (Fig. 7). Again, a zero plate height for the column was assumed and polydispersity data from the manufacturer were used. The polydispersity of toluene was artificially chosen to be 2 in order to obtain a non-zero peak width. The largest PS from the sample (2750 kilodalton) was not included in the calculations because simulating peaks that have minimum τ value (this is at the backward turn of the calibration graph) is more complicated. The theoretical calibration graph, used for simulation, was best fitted to the experimental points for $C=3.3$ at the current linear velocity.

Comparing Fig. 7 with Fig. 6a for low molecular weights reveals that in this range the contribution of polydispersity to the total band broadening is small; the experimental resolution is smaller than that predicted from the polydispersity alone. However, with increasing polymer size, the polydispersity seems more and more responsible for the observed peak widths. Surprisingly, for the highest molecular weights, the experimental resolution is even better than that in the simulated chromatogram. This again shows that the polymer fractions may be of a narrower molecular weight distribution than was suggested by the stated polydispersity data.

HDC of colloids

Some preliminary experiments were carried out to investigate the applicability of HDC to the separation of colloidal silica particles in the size range 1–100 nm. Separations in this size range have already been performed successfully by means of SEC. However, the separation efficiency in SEC for these colloids is poor because of the extremely slow mass transfer between the mobile phase and stagnant phase owing to the very small diffusion coefficients. In HDC on non-porous particles the stagnant phase is absent and a higher efficiency can be expected, provided that adsorption of the

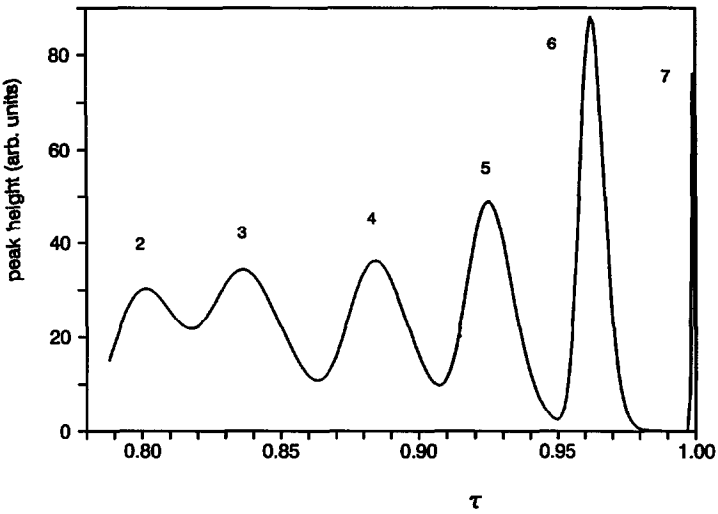

Fig. 7. Simulated chromatogram of PS on column A using eqn. 1 where $C = 3.3$. Same sample as in Fig. 6 except no 2750-kilodalton PS. Polydispersity, M_w/M_n: (2) 1.06; (3) 1.08; (4) 1.05; (5) 1.05; (6) 1.05; (7) 2.0.

colloids can be avoided. Kirkland[37] showed that particle–wall interactions can be kept small when the silica surface and colloidal particles repel each other. This occurs when the pH of the mobile phase is larger than 8. Under these conditions, both the surface of the packing and that of the colloidal particle bear negative charges. These repulsion effects are largest when a thick electrical double layer is present, so a low ionic strength of the mobile phase should preferably be used. Therefore, in our HDC system the aqueous phase contained about 10^{-4} M ammonia to adjust the pH to 8.9. No dissolution of the silica packing was observed during several weeks of operation.

To detect the colloidal particles by turbidity measurement (at a wavelength of 200 nm), replacement of the fused-silica detection tube by a micro-cell with a volume of 2.3 μl was required. This larger detection volume decreased the efficiency of the column by a factor of about two. Fig. 8 shows the HDC of a 14-nm nanosphere and the marker (acetone) on column A. Although the column efficiency is worse with the larger detection cell, the efficiency for both solutes is still very good (plate height *ca.* 10 μm) and is much better than that obtained with SEC.

The τ value of the nanosphere is 0.83, which is significantly smaller than expected on the basis of the aspect ratio. This behaviour must be attributed to the thickness of the double layer existing on both the surface of the packing and the colloid. The presence of the double layer, whose thickness depends on the ionic strength of the mobile phase, narrows the flow channels and enlarges the radius of the colloid, so the aspect ratio increases. The influence of the double layer may have an especially large influence on the aspect ratio when extremely narrow flow channels, such as those in this study, are used. Changing the ionic strength is thus a means of manipulating the retention of colloids in HDC. This aspect is now under investigation.

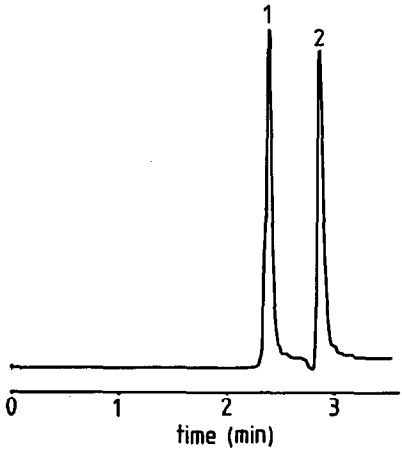

Fig. 8. HDC separation of colloidal silica particles on column A. Eluent: 10^{-4} *M* ammonia (pH 8.9). Sample: 1 = colloidal silica particles 14 nm; 2 = acetone (marker). $\tau_1 = 0.83$.

CONCLUSIONS

(1) Spherical non-porous particles of 1.4–2.7 μm can be efficiently packed in 150–250 × 4.6 mm I.D. columns for HDC.

(2) Reduced plate heights below 2 can be realized when the external band spreading is kept at a level of 1 μl.

(3) Non-porous packings of 1.4–2.7 μm are suitable for the size analysis of polystyrenes by HDC in the molecular weight range 10^4–10^7.

(4) The migration behaviour of polystyrenes up to M_w 10^6 agrees well with the theoretical model described by DiMarzio and Guttman[1,2] for the investigated particle sizes.

(5) For polystyrenes with $M_w > 10^6$ the relative migration (τ) is flow dependent and indicates the occurence of shear degradation.

(6) The application of packed-bed HDC to the analysis of inorganic colloids looks promising.

(7) The high resolving power and the large volume scale of packed-column HDC indicate that the micro-preparative use of this technique is very promising.

(8) It is worth investigating the reduction of the size of the packing particles, the influence of the nature of the solvent and the type of polymer on the elution behaviour in HDC and the applicability of HDC on small spherical porous particles in order to extend the calibration of SEC with HDC.

REFERENCES

1 E. A. DiMarzio and C. M. Guttman, *J. Polym. Sci.*, 7 (1969) 267.
2 E. A. DiMarzio and C. M. Guttman, *Macromolecules*, 3 (1970) 131, 681.
3 H. Small, *J. Colloid Interface Sci.*, 48 (1974) 147.
4 K. O. Pedersen, *Arch. Biochem. Biophys., Suppl.*, 1 (1962) 157.
5 A. W. J. Brough, D. E. Hillman and R. W. Perry, *J. Chromatogr.*, 208 (1981) 175.

6 R. J. Noel, K. Gooding, F. E. Regnier, D. M. Ball, C. Orr and H. E. Mullins, *J. Chromatogr.*, 166 (1978) 373.
7 A. J. McHugh, *CRC Crit. Rev. Anal. Chem.*, 15 (1984) 63.
8 R. Tijssen, J. Bos and M. E. van Kreveld, *Anal. Chem.*, 58 (1986) 3036.
9 K. K. Unger and H. Giesche, *Ger. Pat.*, DE-3534 143.2 (1985).
10 J. C. Kraak, R. Oostervink, H. Poppe, U. Esser and K. K. Unger, *Chromatographia*, 27 (1989) 585.
11 S. Mori, R. S. Porter and J F. Johnson, *Anal. Chem.*, 46 (1974) 1599.
12 M. G. Styring, C.J. Davidson, C. Price and C. Booth, *J. Chem. Soc., Faraday Trans. 1*, 80 (1984) 3051.
13 R. Tijssen, J. P. A. Bleumer and M. E. van Kreveld, *J. Chromatogr.*, 260 (1983) 297.
14 R. F. Stoisits, G. W. Poehlein and J. W. Vanderhoff, *J. Colloid Interface Sci.*, 4 (1976) 549.
15 A. J. McHugh, C. A. Silebi, G. W. Poehlein and J. W. Vanderhoff, *J. Colloid Interface Sci.*, 4 (1976) 549.
16 C. A. Silebi and A. J. McHugh, *AIChE J.*, 24 (2) (1978) 204.
17 D. J. Nagy, C. A. Silebi and A. J. McHugh, *J. Colloid Interface Sci.*, 79 (1981) 264.
18 D. C. Prieve and P. M. Hoysan, *J. Colloid Interface Sci.*, 64 (1978) 201.
19 B. A. Buffham, *J. Colloid Interface Sci.*, 67 (1978) 154.
20 M. Leitzelement, K. Larson and J. Dodds, *Analusis*, 12 (1984) 260.
21 H. Small, F. L. Saunders and J. Solc, *Adv. Colloid Interface Sci.*, 6 (1976)237.
22 R. B. Bird, W. E. Stewart and E. N. Lightfoot, *Transport Phenomena*, Wiley, New York, 1960, p. 197.
23 J. C. Giddings, *J. Chromatogr.*, 5 (1961) 61.
24 J. F. K. Huber, *J. Chromatogr. Sci.*, 7 (1969) 85.
25 Cs. Horváth and H. Lin, *J. Chromatogr.*, 126 (1976) 401.
26 J. H. Knox and F. McLennan, *Chromatographia*, 10 (1977) 75.
27 M. E. van Kreveld and N. J. van den Hoed, *J. Chromatogr.*, 83 (1973) 111.
28 M. E. van Kreveld, *J. Polym. Sci., Polym. Phys. Ed.*, 13 (1975) 2253.
29 H. Brenner and L. J. Gaydos, *J. Colloid Interface Sci.*, 58 (1977) 312.
30 A. M. Basedow, K. H. Ebert and H. Hunger, *Macromol. Chem.*, 180 (1979) 411.
31 H. G. Müler and J. Klein, *Macromol. Chem.*, 182 (1982) 513.
32 J. C. Giddings, *Adv. Chromatogr.*, 20 (1982) 217.
33 J. C. Giddings, *Sep. Sci.*, 13 (1978) 241.
34 A. Rudin, *J. Polym. Sci. Part A-1*, 9 (1971) 2587.
35 M. Fixman and J. M. Peterson, *J. Am. Chem. Soc.*, 86 (1964) 3521.
36 J. C. Moore, *Sep. Sci.*, 5 (1970) 723.
37 J. J. Kirkland, *J. Chromatogr.*, 185 (1979) 273.